# Study of the spatial resolution achievable with the BTeV pixel sensors

Marina Artuso and Jianchun Wang

*Department of Physics, Syracuse University, Syracuse, NY 13244*

**Abstract**

A Monte Carlo simulation has been developed to predict the spatial resolution of silicon pixel detectors. The results discussed in this paper focus on the unit cell geometry of 50 $\mu$m $\times$ 400 $\mu$m, as chosen for BTeV. Effects taken into account include energy deposition fluctuations along the charged particle path, diffusion, magnetic field, and response of the front end electronics. We compare our predictions with measurements from a recent test beam study performed at Fermilab.

*Key words:* Pixel; Silicon;

## 1 Introduction

BTeV is an experiment designed to explore heavy flavor phenomenology thoroughly [1], with particular emphasis on mixing, $CP$ violation and rare and forbidden decays. The pixel detector system is crucial to the experiment. We have engaged in a thorough study of several different factors influencing the sensor performance, with particular emphasis on spatial resolution and detector occupancy. As the radiation dose is very intense at small distances from the beam axis, our main emphasis is on $n^+np^+$ sensors [2], where the collected charge carriers are electrons.

We report the most important results on the expected performance of the BTeV baseline front end-sensor systems, as well as a comparison between our predictions and results recently obtained in a test beam run that took place at Fermilab, where we took extensive data using different prototype sensors and readout electronics [3].

## 2 Spatial resolution studies

We have investigated several factors affecting the spatial resolution, in particular charge diffusion, magnetic field, electronic noise, discriminator threshold and digitization resolution.

We have modeled the signal induced by minimum ionizing tracks traversing silicon using a charge straggling distribution function supported by experimental data and a detailed theoretical model of the interactions responsible for the energy loss in silicon [4]. The detector has been conceptually divided into $\sim 30$ $\mu$m thick slices to model fluctuations in the energy deposition along the charged particle track path. The most probable charge signal produced by a minimum ionizing particle in the 280 $\mu$m p-stop sensors used in the test beam data is found to be 24000 $e^-$ with a full width at half maximum of 10000 $e^-$, in good agreement with the corresponding parameters of the measured distribution [3].

Electrons and holes produced by the energy deposited by a traversing charged particle drift along the electric field lines ($\vec{E}$) in the detector. The equations describing this drift motion are:

$$\vec{J_e} = -q\rho_e\mu_e\vec{E} \tag{1}$$

$$\vec{J_h} = q\rho_h\mu_h\vec{E} \tag{2}$$

where $q$ is the magnitude of the electron charge, $\mu_e$ and $\mu_h$ are the mobility of electrons and holes respectively, $\rho_e$ is the number of free electrons per unit volume, and $\rho_h$ is number of free holes per unit volume.

The charge cloud spreads laterally due to diffusion. The parameters characterizing the drift in the electric field ($\mu_h$, $\mu_e$) are related to the parameter describing the diffusion of the charge cloud ($D_h$,$D_e$) by the Einstein equation:

$$D_{h(e)} = \frac{kT}{q}\mu_{h(e)} \tag{3}$$

where $D_h$ and $D_e$ are the diffusion coefficients and $kT$ is the product of the Boltzmann constant and the absolute temperature of the silicon. The average square deviation with respect to the trajectory of the collected charge without diffusion is $< \Delta r^2 >= 2D\Delta t$. In our study we have used $\mu_h = 400$ cm$^2$/Vs, $\mu_e = 1450$ cm$^2$/Vs [5]. A magnetic field perpendicular to $\vec{E}$ produces a distortion of the collected charge distribution parameterized in terms of the Hall mobility $\mu_H$, proportional to the drift mobility. Finally, the charge-cloud is collected on more pixels when the incident track crosses the

detector at an angle, as the generation points of the electron-hole pairs spread out along the track path. These various effects are illustrated in Fig. 1 as a function of the incident angle $\theta$.

The discriminator threshold also influences the spatial resolution. In this study we have assumed that only the pixels having a signal above threshold are read out, and we have varied the threshold for analog and binary readout. Fig. 2 (top) shows the effect of increasing the threshold for an incident angle $\Theta = 300$ mr, for analog and digital readout respectively. The bottom plot shows the fraction of events having $N$ pixels hit for a given threshold. For instance, for a threshold of 1000 electrons, about 60% of the events have 3 pixels hit, and about 40% have 2 pixels hit. The resolution achievable for binary readout shows a characteristic oscillatory behavior as we change the threshold. As the digital clustering algorithm exploits the information provided by the number of pixels in a cluster, its accuracy is best when there is an almost equal population in two different cluster sizes: the smaller cluster corresponding to a track incident in a pixel center and the bigger cluster corresponding to incidence close to the boundary between two pixels. In the analog readout case, the accuracy of any position reconstruction algorithm is degraded as the threshold increases.

A pixel detector has the potential for being a very low noise system, since the capacitive load at the input of the charge sensitive preamplifier is negligible. We have achieved [6] 100 $e^-$ noise or below on the test bench. In order to take full advantage of the low noise, the minimum threshold spread among channels needs to be small. The measured spread in the devices used in the test beam run is about 380 $e^-$ [3]. Prototypes of the more advanced version of this design show that a threshold spread of 180 $e^-$ or better is achievable. Therefore noise and threshold spread figures are not a limiting factor in the detector performance.

An analog readout is a preferred solution for several reasons, including more effective monitoring of the stability of the detector properties and improvement in the spatial resolution. We need to know how many bits are required because the analogue circuit must fit within the small pixel cell boundary. Furthermore, we need to extract the digitized information very quickly. We have thus investigated several different combinations of ADC transfer functions, varying both the dynamic range and the digitization accuracy. Fig. 3 shows an example where the expected performance of our analog front end electronics combined with a logarithmic 3 bit flash ADC is shown. As a comparison, the resolution expected from a 8 bit linear ADC is included. Note that the difference is not too dramatic. This supports our conclusion that the digitization resolution of 3 bits, chosen for our front end electronics, FPIX2, is optimal for our application.

In order for this simulation tool to be effective, its accuracy must be checked with experimental data. We have done a systematic study of the performance expected from various sensor and readout electronics combinations used in the recently completed test beam run. Details on the data taken and the analysis procedure are given elsewhere in these proceedings [3]. The comparison between predicted and measured resolution is shown in Fig. 4 for two different digitization accuracies (8 bit and 2 bit ADCs) as well as binary readout. The data for the two ADCs tested were taken with different thresholds. Fig. 4 includes a simulation of the 2 bit ADC case with the lower threshold, showing that the higher threshold used with the coarser ADC resolution is a dominant effect, in particular at small incidence angles. The agreement with the data is very good, especially if we take into account that factors like imperfect alignment, track projection errors and angular resolution have not yet been included.

## 3 Conclusions

The Monte Carlo simulation algorithm discussed in this paper has been a key element in our optimization of the baseline design of the BTeV pixel detector system. The good agreement with recent test beam data gives us confidence that the most important factors affecting the pixel performance are modeled accurately and that this baseline design will be an excellent tool to achieve our physics goals.

While the results presented here are specific to the BTeV experiment, the algorithm developed is quite general and can be applied to other detector systems.

## 4 Acknowledgements

We thank D. Christian, S. Kwan, R. Mountain and S. Stone for interesting discussions. MA thanks the organizers for a very informative workshop, in a beautiful setting. This work was supported by the U.S. National Science Foundation.

## References

[1] The BTeV Collaboration, *The BTeV Proposal* (2000); http://www-btev.fnal.gov/public_documents/btev_proposal/.

[2] R. Horisberger, *Nucl. Instr. Meth.* **A384** (1996) 185.

[3] G. Chiodini, *These proceedings.*

[4] H. Bichsel *Rev. Mod. Phys.* **60** (1988) 663.

[5] L.H.H. Scharfetter (RD19), *Active Pixel Detectors for Large Hadron Colliders*, CERN Thesis, (1997).

[6] A. Mekkaoui, *These proceedings.*

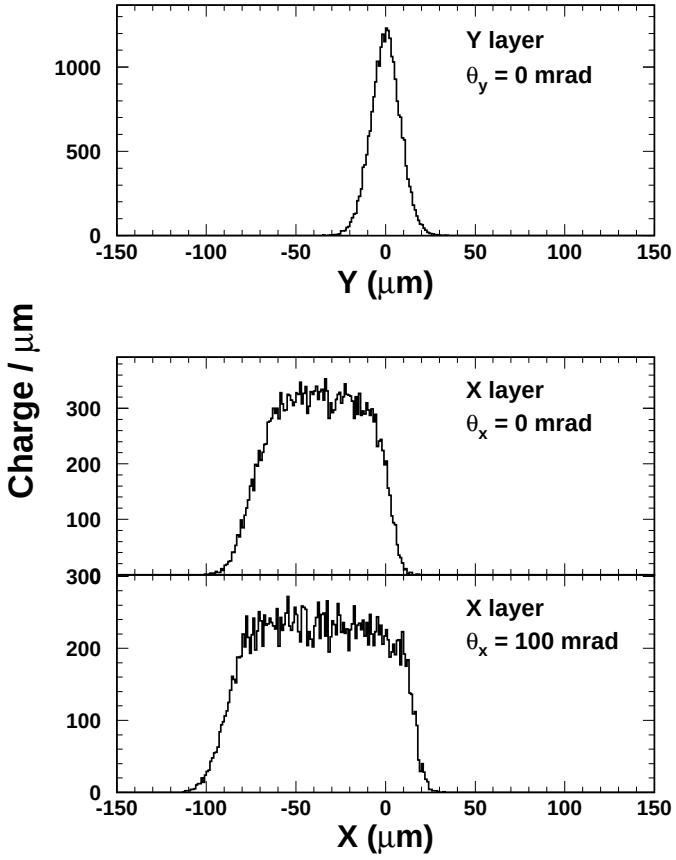


Fig. 1. Collected charge spreading in a 280 $\mu$m silicon detector a) produced by diffusion (the label Y layer identifies a pixel sensor oriented with the small pixel dimension parallel to the magnetic field); b) produced by the interplay of diffusion and the magnetic field for B=1.6T, and c) produced by diffusion and magnetic field effects when the charged track is incident at an angle of 100 mr in the bend plane (the label X layer identifies a pixel sensor oriented with the small pixel dimension perpendicular to the magnetic field).

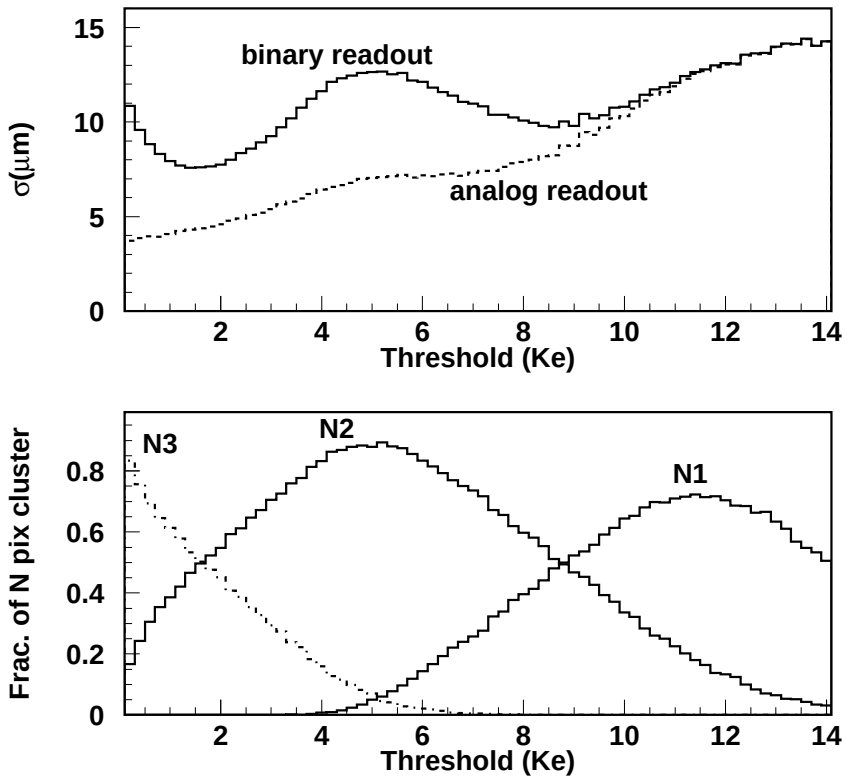


Fig. 2. a) Spatial resolution in the reconstructed x coordinate as a function of the threshold for a pixel size of 50 x 400 $\mu$m$^2$ and incidence angle of $\theta$ = 300 mr. b) Percentage of events having N pixels hit as a function of the threshold for the same configuration. No magnetic field is applied in this simulation.

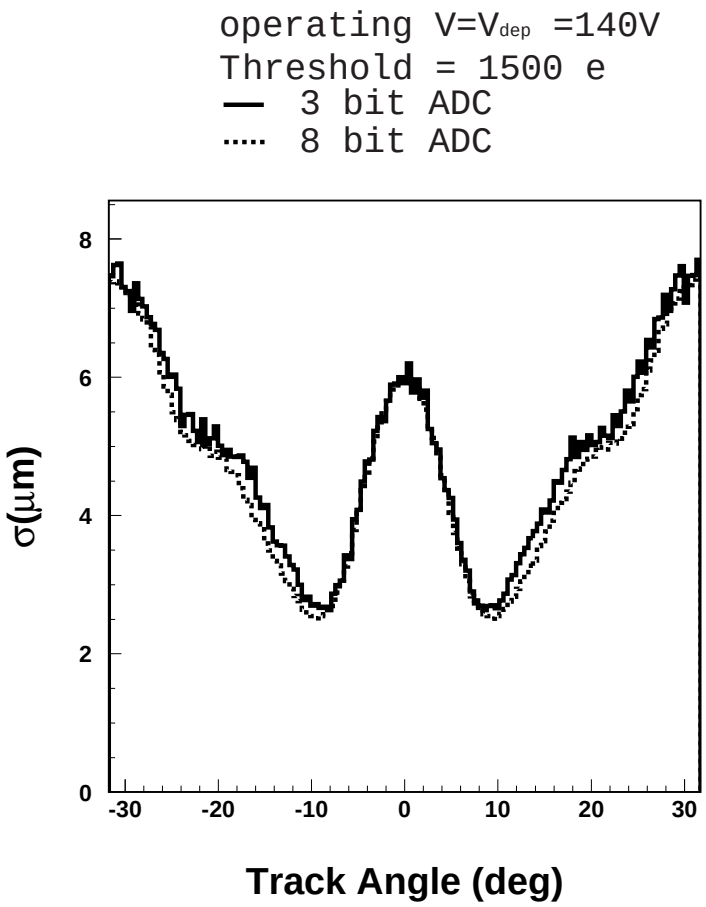


Fig. 3. Sensitivity of the spatial resolution in the reconstructed x coordinate to the digitization resolution. A logarithmic 3 bit ADC (FPIX2) is compared to a linear 8 bit ADC. The threshold is assumed to be 1500 $e^-$, with a dispersion of 200 $e^-$. The maximum dynamic range is assumed to be 20000 $e^-$. The sensor is biased at the depletion voltage (assumed to be equal to 140 V) and has a thickness of 250 $\mu$m.

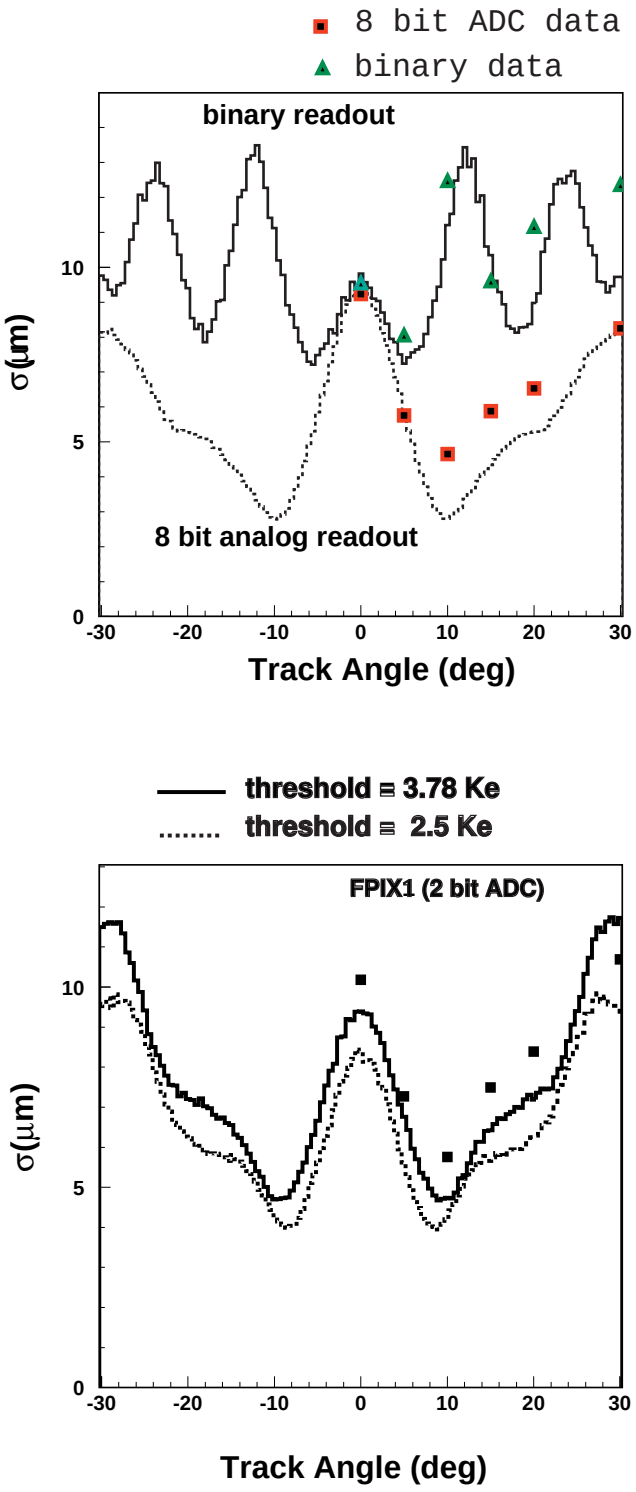


Fig. 4. Comparison between Monte Carlo predictions (curves) and test beam data (points); top: FPIX0 data (8 bit ADC external to front end chip, the curve labeled 'binary' corresponds to the same data analyzed using only the pixel over threshold information; bottom: FPIX1, (2 bit ADC).